TESTING AND MODELLING OF TENSION AFTER IMPACT OF A THIN PLY TEXTILE COMPOSITE

Robin Olsson[1], Fredrik Ahlqvist[1], Alann André[1], Peter Hellström[1], Elena Alvarez[2], Emilio V. González[3], Jose Ramon Sainz de Aja[4], Federico Martín de la Escalera[4]

[1]Swerea SICOMP, SE-431 22 Mölndal, Sweden
Email: robin.olsson@example.com, fredrik.ahlqvist@swerea.se, alann.andre@swerea.se, peter.hellstrom@swerea.se, Web Page: http://www.swerea.se/en/sicomp
[2]Oxeon AB, Företagsgatan 24, SE-504 64 Borås, Sweden
Email: elena.alvarez@textreme.com,Web Page: http://www.textreme.com
[3]AMADE, EPS - Universitat de Girona, Campus Montilivi s/n, 17071 Girona, Spain
Email: emilio.gonzalez@udg.edu, Web Page: http://www.amade.udg.edu
[4]Aernnova Engineering Division,Avd Manoteras 20 edif B 5º Planta, 28050 Madrid
Email: joseramon.sainzdeaja@aernnova.com, federico.martindelaescalera@aernnova.com,
Web Page: http://www.aernnova.com/en/

Keywords: thin plies, impact, damage tolerance, testing, finite element model

Abstract

This paper presents an experimental and numerical study of impact response, damage and tension after impact of thin ply HTS45/RTM6 carbon/epoxy laminates, manufactured via resin transfer moulding. A plain weave from carbon fibre spread-tow bands was used in a quasi-isotropic layup. Finite element simulations were performed using layered shell elements accounting for in-plane damage mechanics, with cohesive surfaces between a few layers of shell elements to account for delamination. The damage was found to include a combination of fibre damage and delaminations, in contrast to a previous study on similar cross-ply laminates, where fibre damage dominated. The rate of decrease in tensile strength after impact was similar to prepreg laminates with conventional ply thickness, but the impacted strength was slightly higher due to a higher undamaged strength for thin ply laminates.

1. Introduction

Matrix cracking in multidirectional laminates occurs by constrained crack growth along the fibres. By reducing the ply thickness the crack growth can be suppressed or delayed. Hence, thin ply composites offer higher strains to first ply failure and higher ultimate strength. This capability is attracting great interest from the aircraft industry, and has been demonstrated in a number of studies, e.g. [1, 2]. A potential concern is, however, that a smaller interval between first ply failure and ultimate failure might cause increased notch sensitivity and reduced damage tolerance, e.g. after impact.

Textile preforms impregnated with resin, e.g. by resin transfer moulding (RTM), offer increased speed in production compared to traditional manufacture with prepreg and autoclaving. Furthermore the problems with storage and limited shelf life can be eliminated. A drawback is, however, reduced mechanical properties due to the crimp of fibres. The crimp may be reduced by thinner plies.

Laminates made by impregnation of thin ply weaves, e.g. TeXtreme®, made from spread tow bands combine the advantages in cost and manufacturing speed of textiles with the higher mechanical performance and reduced matrix cracking of thin plies. The performance and viability of the

Excerpt from ISBN 978-3-00-053387-7

TeXtreme® material for aircraft structures has been examined in a number of studies, [3, 4]. Impact resistance and impact damage was studied for 100 gsm (g/m^2) cross-ply laminates with an epoxy resin, cured at 80°C [4]. This study indicated that damage is dominated by fibre fracture and occurs by bending failure by "folding" along the major axis of rectangular plates. An analytical model was developed to explain the failure mechanism and predict the failure initiation [5], while a finite element (FE) model based on shell elements with in-plane damage mechanics was used to predict the damage growth [4].

The current paper presents an experimental and computational study of the impact damage tolerance of quasi-isotropic 80 and 160 gsm TeXtreme® laminates impregnated by RTM6 and cured at 180°C, as used in the aircraft industry. Tension after impact (TAI) is studied as it may be significantly reduced by fibre damage. Compression after impact is not covered in this paper but was studied by the Spanish partners of the project. A related paper has also studied the load-deflection curve and damage sequence of identical laminates and boundary conditions under static loads at the impact point [6].

2. Experiments

2.1. Specimens and material

Specimens were manufactured from TeXtreme® plain weave by Oxeon made from unidirectional (UD) spread tow bands of HTS45 carbon fibres impregnated with RTM6 epoxy resin, with a T_g of 195°C. 80 and 160 gsm (g/m^2) weaves were used, corresponding to a ply thickness of 0.08 and 0.16 mm, i.e. a band thickness of 0.04 and 0.08 mm. The plates were manufactured by Aernnova using RTM, with two in-plane injection points at the centre of the long edges, and one out-of-plane vent point at the centre of the plate. The injection pressure was 1 bar for 1 min and then gradually increased up to a constant pressure of 3 bars. The injection temperature is at mould temperature of 120ºC. The curing consisted of a temperature ramp of 1-3 ºC/min during 90 minutes up to 180ºC, at a constant pressure of 3 bars. The binder was activated at temperature 40ºC, and in all the preform the binder was activated ply by ply up to obtaining the compacted preform. After manufacture all specimens were ultrasonically inspected for defects, and some specimens from regions with dry spots were discarded.

All specimens had a quasi-isotropic layup and a nominal thickness of 4.48 mm. The layups were $[(45/\text{-}45)/(0/90)]_{14s}$ for the 80 gsm weave and $[(45/\text{-}45)/(0/90)]_{7s}$ for the 160 gsm weave, where the numbers within curved brackets correspond to the bands in a single weave ply. The in-plane dimensions were 150x100 mm for the specimens used for damage studies, and 320x100 mm for the specimens to be tested in tension after impact (TAI).

The mechanical properties of unidirectional plain weave (with equal amounts of UD bands in the 0° and 90° directions) were tested in separate tests at AMADE - University of Girona. For the present modelling all properties were re-calculated by fitting to equivalent properties of the individual UD bands, as each weave ply was modelled as a sublaminate with perpendicular UD layers. G_{c1T}, G_{c1C}, G_{c2T} and G_{c2C} are in-plane toughness values in directions 1 and 2, in tension (T) and compression (C).

Table 1. Mechanical properties of UD bands in 80 gsm TeXtreme®-weave. *= In-situ property, c.f. [4]

	E_1	$E_2 = E_3$	$G_{12} = G_{13}$	G_{23}	$\nu_{12}=\nu_{13}$	ν_{23}
[GPa]	117	10	4	3	0.3	0.45
	X_t	X_c	Y_t	Y_c	S_L	S_T
[MPa]	2000	1337	275*	146	124*	124*
	G_{c1T}	G_{c1C}	G_{c2T}	G_{c2C}	G_{Ic}	G_{IIc}
[kJ/m^2]	118	26 [5]	0.5	1.1$^{\text{assumed}}$	0.5	1.1

Excerpt from ISBN 978-3-00-053387-7

2.2. Impact testing

Drop weight impact tests were performed according to the standard ASTM D7136/D7136M-12. The specimens were placed on a support frame with a 125x75 mm or 75x75 mm window and impacted centrally at nominally 20 J (2.8 m/s) or 30 J (3.4 m/s) using a 5.124 kg mass with 8 mm tup radius. The square window was used for a few specimens to investigate differences in damage when bending strains were equal in the *x*- and *y*-direction. The specimens were lightly clamped with rubber tipped clamps at the corners of the window, allowing virtually simply supported edge conditions.

The impact load was recorded using a Dytran 1203V5 piezoelectric load sensor connected to a Dytran 4102C current source, and the back face deflection was recorded using a MEL M70LL/10 laser displacement sensor. Furthermore, the impact velocity immediately before impact was measured by the passage time of a 4 mm diameter steel pin through an optical gate, which allowed accurate calculation of the actual impact energy. All signals were recorded on a PicoScope 4424 four channel digital oscilloscope, and post-processed using a standard PC.

2.3. Fractography

After impact all specimens were ultrasonically C-scanned using a handheld Sonatest Rapid Scan 2 rolling type scanner, to determine size, shape and depth of the delaminations generated by the impact.

Some specimens were sectioned along the length or width axes, potted in epoxy with a fluorescent dye, polished and examined in an optical microscope. The fluorescent epoxy allowed cracks and cavities caused by the impact to be clearly distinguished from resin rich areas generated during manufacture. This allowed detailed mapping of matrix cracks and delaminations in specific sections.

Other specimens were placed in a furnace to burn away most of the resin, which allowed separation of the plies. After deplying every ply was scanned in a high resolution document scanner and the observed fibre cracks were manually highlighted in digital images. Each ply was scanned on the upper and lower side to record cracks in both the 0° and 90° bands. This allowed a detailed mapping of the fibre cracks in all plies of the laminate.

2.4 Tension after impact

After impact and ultrasonic inspection the specimens for tension after impact (TAI) were equipped with 50 mm long tabs and mounted in a Dartec 600 kN test machine with hydraulic grips at Luleå University of Technology. The gripping force was set to 300 kN, and tests were done at a constant displacement rate of 2 mm/min. Load and displacement were recorded at a rate of 10/s.

Strains in undamaged specimens were measured with a 50 mm extensometer. For impacted specimens full field 3D measurement of displacements and strains was performed at 3 frames/s using a GOM Aramis 2M digital image correlation (DIC) system with Aramis software v6.2.0. Displacements were measured in a region of 44 mm width and 60 mm height. The applied strain was defined as the average value in this region, excluding a small central region with singular strains, caused by fibre cracks.

3. Finite element modelling

The impact analysis was run in ABAQUS using the Implicit/Dynamic solver. The TAI simulation was performed in ABAQUS/Standard (Static Analysis) using the damage state at the end of the impact simulation as an initial condition, imported as a material state (Predefined Field/Initial State).

The laminate was modelled with layered continuum shell elements, where each ply in the laminate was modelled as two perpendicular UD-layers in the directions 0°/90° or +45°/-45. Thus the 80 gsm laminate was modelled with 112 UD layers and the 160 gsm with 56 layers. An initial study of a

Excerpt from ISBN 978-3-00-053387-7

checker board layup, where 0° and 90° plies alternated for each weave square, provided virtually identical results, and hence this more complicated approach was abandoned.

The available bilinear damage mechanics law with Hashin's failure criteria for in-plane damage initiation was used for each layer. Delaminations were initially excluded from the model and a single shell element was used for the entire laminate, but the predicted damage and response deviated somewhat from the experiments. For this reason simulations were also performed with 3, 5 or 9 shell elements through the thickness, connected by 2, 4 or 8 cohesive surfaces with a linear traction-separation softening branch allowing for delamination in peel (mode I) or shear (mode II or III). In addition to the linear elastic properties in Table 1 a nonlinear shear behaviour was included in the model, by fitting a continuous function to experimental data, using the method described in [4].

4. Results and discussion

4.1. Observed impact response and damage

Due to the relatively large impactor mass the impact response in these tests is essentially quasi-static, i.e. the load-deflection history is similar to what would be observed for a corresponding static test. For this reason all results were plotted with load vs back face deflection, as recorded in the impact tests. This presentation simplifies evaluation of energy consumed during the impact, and identification of loads and deflections associated with particular failure events. Figure 1 gives a comparison between a typical response at 30 J impacts for laminates with 80 and 160 gsm plies. The deflection obtained at 20 J impacts has been included for comparison. It is obvious that the response for 80 gsm and 160 gsm laminates is relatively similar for impact energies up to about 25 J, but significantly different at higher energies.

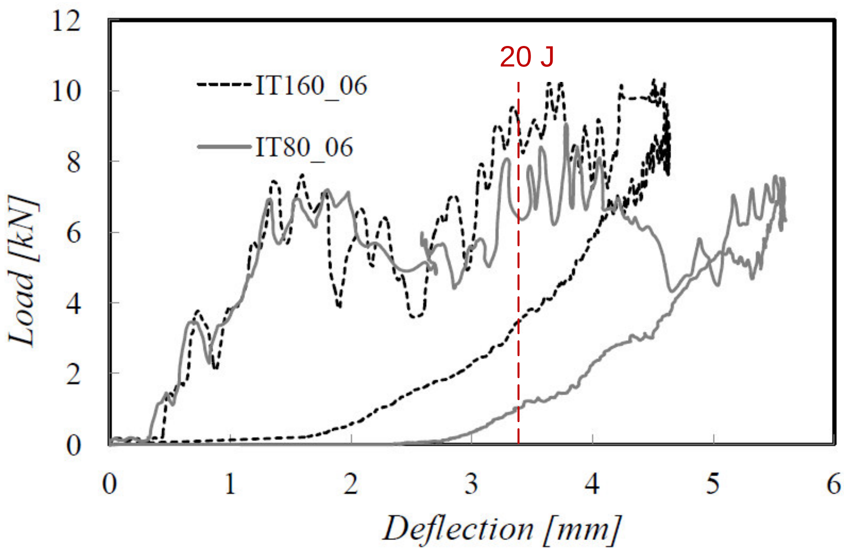

Figure 1. Typical load-deflection for an 80 and 160 gsm laminate impacted at 30 J.

Delamination zones at 20 J were similar and relatively circular for the 80 and 160 gsm laminates, in agreement with the similar impact response, Fig. 2. At 30 J the delamination zones were more different, with a more extended delamination zone for the 80 gsm laminate, somewhat similar to what was previously observed for a cross-ply 100 gsm TeXtreme® laminate with LY556 epoxy resin [4].

Excerpt from ISBN 978-3-00-053387-7

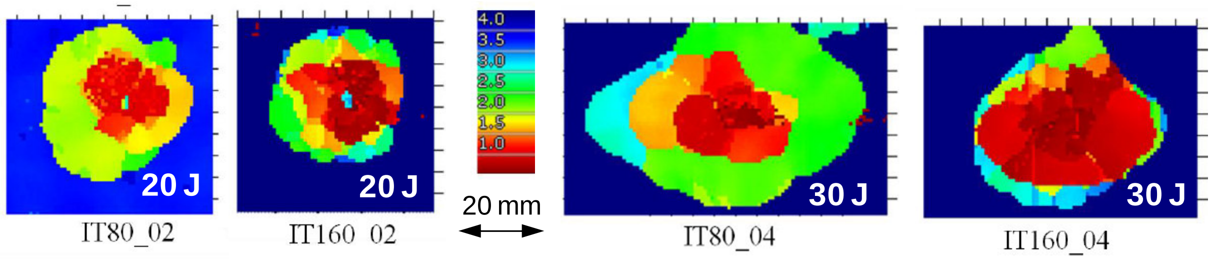

Figure 2. Differences in delaminations in 80 and 160 gsm laminates impacted at 20 and 30 J.

The extended delamination zone for the 80 gsm laminate at 30 J was linked to extensive fibre along the major axis of the laminate, Fig. 3 (left), which is assumed to be the cause for the load drop at 4 mm deflection in Fig. 1. Similar but more pronounced effects were observed for the 100 gsm laminate in [4]. In contrast the fibre damage zone in the 160 gsm laminate was localized to a small central region, in agreement with previous observations for quasi-isotropic pregreg laminates with conventional ply thickness, [7]. The distribution of fibre crack lengths through the thickness was mapped for each ply after deplying, and is presented in Fig. 3 (right). It is noted that the damage width is uniform, or increases towards the back face, which is typical for failure by membrane stresses. This type of failure indicates that delamination preceded fibre fracture. In contrast the cross-ply laminates in [4] had an hour glass distribution of fibre failure through the thickness, which indicates that bending failure preceded delamination. It is unclear whether this difference was caused by the cross-ply layup, or by a higher interlaminar toughness. The earlier delamination in the current laminates may also have been caused by the higher cure temperature (180°C instead of 80°C) which generates larger residual stresses and promotes earlier matrix cracking that may trigger delaminations.

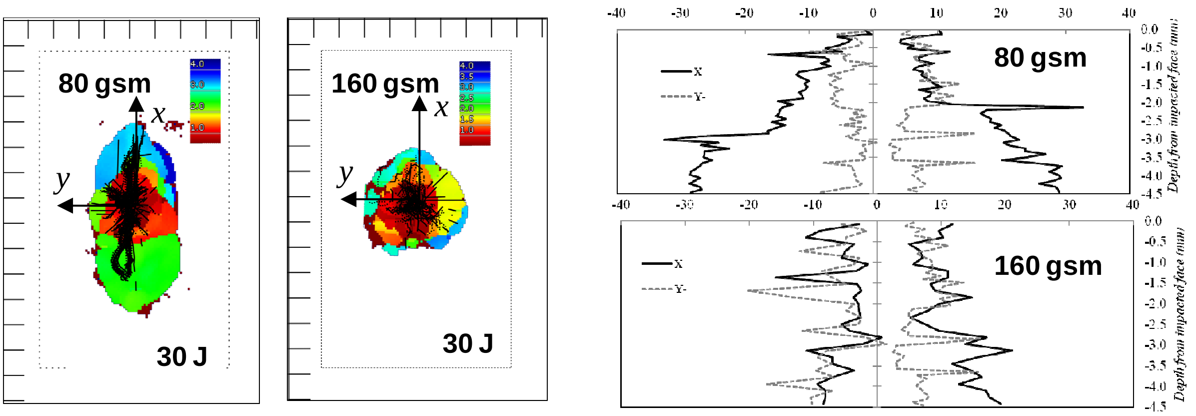

Figure 3. In-plane and through-thickness distribution of fibre cracks in the laminates.

4.2. Predicted impact response and damage

The FE model with layered shells and in-plane damage mechanics that had previously successfully been applied to 100 gsm cross-ply TeXtreme® laminates was also applied to the current tests on 80 and 160 gsm quasi-isotropic laminates, but the predicted response differed significantly from the experiments. Delaminations appeared earlier and were considerably more prominent, which obviously affects the response significantly. For this reason a limited number of delaminations (2, 4 or 8) were included in the FE-model, by dividing the laminate in 3, 5 or 9 equally thick sublaminates. Figure 4 compares experimental results with FE simulations without (No Hashin) and with (Hashin) in-plane damage. It is evident that delaminations are required for a correct description of the response, but a larger number of cohesive surfaces causes a decreasing delamination threshold load and an artificial increase in the plate compliance. Furthermore, the introduction of cohesive surfaces appeared to affect the in-plane failure in an unexpected way. The cause for this effect is unclear but may possibly be an uneven partitioning of the sublaminates in the laminates.

Excerpt from ISBN 978-3-00-053387-7

Figure 5 shows observed in-plane damage and comparisons with predictions from an FE model without delaminations. It is noted that the predicted length of fibre cracks in the *y*-direction is larger for laminates impacted over a square window, as observed in experiments. The predicted in-plane damage was similar when delaminations were included in the model, although the cracks were slightly more concentrated to a small central region. Figure 6 shows the predicted shape of the delamination zone with 2, 4 and 8 delaminations. It is clear that the size of the zone decreases as more delaminations are included in the model.

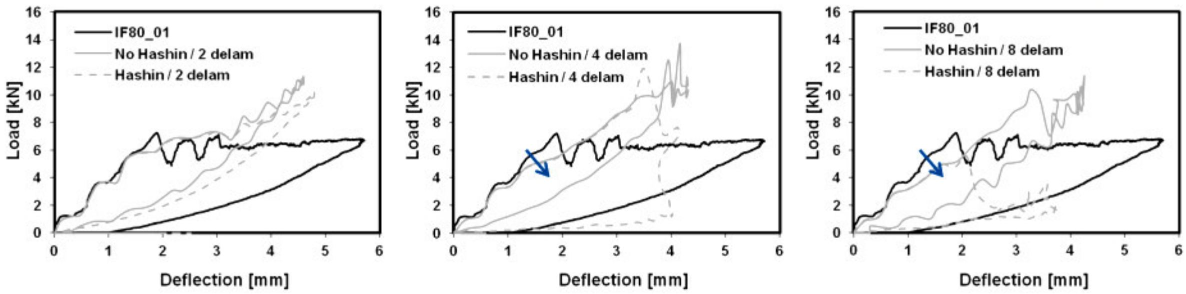

Figure 4. Measured and predicted response for 2, 4 and 8 delaminations without/with inplane damage.

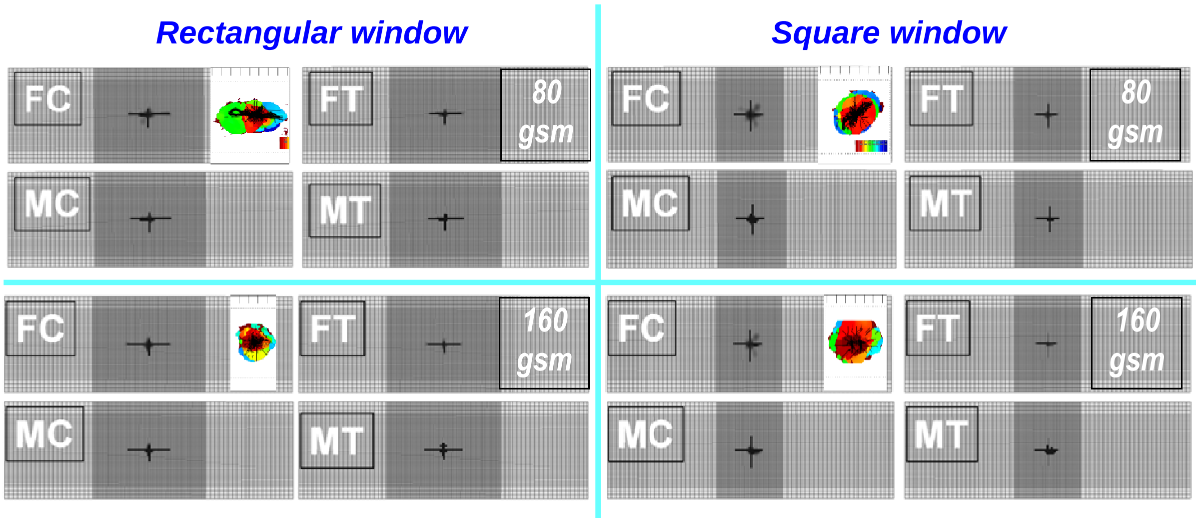

Figure 5. Predicted and observed ply damage in laminates impacted at 30 J.
(FC/FT=fibre compression/tension, MC/MT=matrix compression/tension)

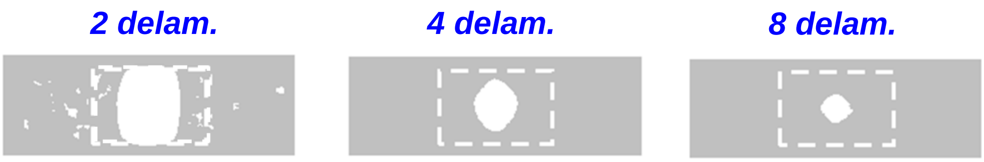

Figure 6. Predicted delaminations in an 80 gsm laminate impacted at 30 J.

4.3. Observed tensile failure after impact

During tensile loading a strain concentration was observed in all specimens, as exemplified in Fig. 7. The strain concentration was higher for specimens impacted at higher energy, and for specimens impacted over a square window rather than a rectangular window. The relation between applied (average) stress and strain was more or less linear almost until final failure. All specimens failed along a straight line across the width of the specimen through the damaged zone. The failure appears to have been initiated by fibre damage causing high local strains, which were visible in the DIC measurements.

Excerpt from ISBN 978-3-00-053387-7

The undamaged strength was higher for the 80 gsm laminates but dropped somewhat faster with impact energy than for the 160 gsm laminates, Fig. 8. Thus, the 80 gsm laminates demonstrated a more brittle behaviour than the 160 gsm laminate, as expected. It was also noted that the strength of the 80 gsm laminates impacted over a square window was much lower than for the ones impacted over a rectangular window, while the effect was very moderate for the 160 gsm laminates. This observation highlights that the TAI strength is linked to the width of fibre cracks perpendicular to the loading direction. Results for a quasi-isotropic laminate from conventional AS4/8552 UD prepreg have been included in Fig. 8 for comparison. The strength of the AS4 fibres is similar to the HTS45 fibres in TeXtreme® and 8552 is similar or tougher than RTM6. In spite of the faster decay in TAI strength of the 80 gsm material it outperforms the AS4/8552 material with conventional thickness, due to a higher undamaged strength. The results for the 160 gsm material indicate, however, that fibre bands of intermediate thickness may provide an optimum damage tolerance.

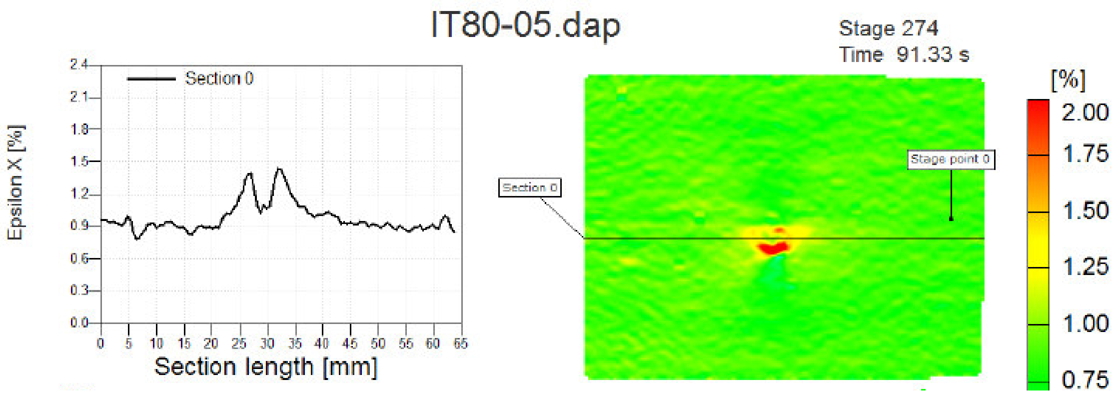

Figure 7. Strain distribution in 80 gsm laminate impacted at 30 J.

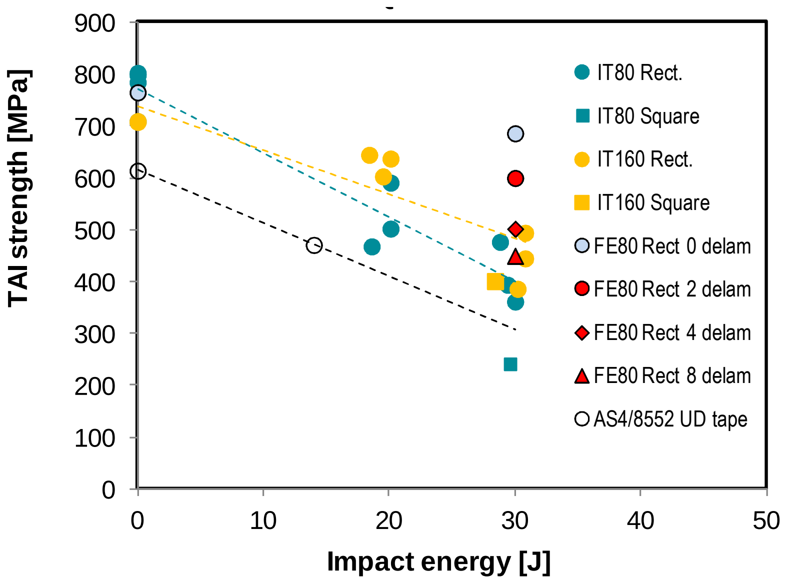

Figure 8. Measured and predicted tensile strength versus impact energy.

4.4. Predicted tensile failure after impact

The predicted behaviour in tension after impact was almost linear up to a sudden failure, which is controlled by the severity of the initial damage. Comparisons between predicted and measured strength (applied average stress at failure) of the 80 gsm laminate impacted at 30 J are given in Fig. 8. It was noted that exclusion of delaminations in the FE model resulted in a severe overestimation of the tensile strength after impact, and that the predictions approached the experimental results

Excerpt from ISBN 978-3-00-053387-7

asymptotically for an increasing number of delaminations. This observation is supported by the detailed FE simulations in [8], where it was shown that delaminations are vital for providing the correct stress concentration from fibre breakage. The small or negligible influence of mere fibre cracks is a result of the shear lag effect, where stress concentrations from broken plies vanish within a few ply thicknesses, due to the influence of interlaminar shear stresses. When delaminations are present this effect is cancelled.

5. Conclusions

Thin ply laminates have a higher undamaged strength than laminates with plies of conventional thickness, but are inherently somewhat more brittle as premature damage growth is suppressed. This implies that they may be more sensitive to e.g. impact, but the tensile strength of the quasi-isotropic laminates impacted at 20 and 30 J in the present study is likely to be higher than for laminates of the same material with thicker plies, due to a higher undamaged strength. A concern may be major fibre cracks *perpendicular* to the load, e.g. for tensile loading across the width of a rectangular laminate, or in any direction of a square laminate. Such loads are not tested for standard specimens, but are likely to occur in applications. It appears that there may exist an intermediate ply thickness for optimal damage tolerance, i.e. the thinnest possible ply may not provide the highest strength after impact.

A previous study on 100 gsm cross-ply laminates cured at 80°C indicated that damage in thin ply laminates is dominated by fibre fracture, while the present study of quasi-isotropic 80 and 160 gsm laminates cured at 180°C indicated an interaction between fibre fracture and delaminations. This implies that both in-plane damage and delaminations need to be included in the model, which is computationally very demanding due to the large number of interfaces. Future work should focus on how this interaction can be accounted for in a sufficiently accurate and computationally efficient way.

Acknowledgments

This work was performed within the DAMTEX project, funded by the European program Air Transport Net (AirTN) through VINNOVA in Sweden and CDTI in Spain. Project partners were Swerea SICOMP (coordinator) and Oxeon in Sweden and Aernnova in Spain, while AMADE/University of Girona was a subcontracted research provider.

References

[1] Yokozeki T, Kuroda A, Yoshimura A, Ogasawara T, Aoki T. Damage characterization in thin-ply composite laminates under out-of-plane transverse loadings. *Compos Struct*, 93(1):49-57, 2010.
[2] Amacher R, Cugnoni J, Botsis J, Sorensen L, Smith W, Dransfeld C. Thin ply composites: Experimental characterization and modeling of size-effects. *Compos Sci Technol*, 101:121-132, 2014.
[3] Marklund E, Asp LE, Olsson R, Ohlsson F, Varna J. Experimental investigation and modeling of thin band woven composites. *TEXCOMP-11*, Leuven, 2013.
[4] Olsson R, André A, Hellström P. Analytical modelling and FE simulation of impact response and damage growth in a thin-ply laminate. Paper 5217-2. *Proc. 20th Int Conf on Composite Materials ICCM-20*, Copenhagen, 19-24 July 2015.
[5] Olsson R. Analytical prediction of damage due to large mass impact on thin ply composites. *Composites Part A*, 72:184-191, 2015.
[6] Wagih A, Maimí P, González EV, Blanco N, Sainz de Aja JR, de la Escalera FM, Olsson R, Alvarez E. Damage sequence in thin-ply composite laminates under out-of-plane loading. *Composites Part A*, 87:66-77, 2016.
[7] Sztefek P, Olsson R. Tensile stiffness distribution in impacted composite laminates determined by an inverse method. *Composites Part A*;39(8):1282-1293, 2008.
[8] Craven R, Sztefek P, Olsson R. Investigation of impact damage in multi-directional tape laminates and its effect on local tensile stiffness. *Compos Sci Technol*;68(12):2518-2525, 2008.

Excerpt from ISBN 978-3-00-053387-7